ROZPRAWY INŻYNIERSKIE • ENGINEERING TRANSACTIONS • 24, 4, 809—818, 1976
Polska Akademia Nauk • Instytut Podstawowych Problemów Techniki

ANALYSIS OF IMPACT DEFORMATION OF CORRUGATED AND ANISOTROPIC SHELLS

B. A. GORDIENKO (CHABAROVSK)

The existence of material anisotropy (at $E_2/E_1 < 1$) in the shells subjected to impact loaying lowers the critical time and leads to axi-symmetric forms buckling. The data of experiments performed on the longitudinally corrugated shells connfirm the theoretical results obtained.

The structurally anisotropic shells and shells made of physically anisotropic materials have broad application in various fields of technology and architecture. In a series of Russian and foreign papers (e.g. [1–11]) the general theory of shells is developed; many papers are devoted to statics and vibrations. The resonance of shells to high intensity transient loads is a domain much less explored. Among papers representing this direction of research let us mention [12–19].

The behaviour of anisotropic shells subjected to dynamic internal pressure is considered in [12–14] and to axial impact—in [15–19]. The theory of shallow shells is studied in papers [15–17]. In [18] the experiments of impact of plastic glass shells are described. The results concerning impact buckling of corrugated shells are presented in [19].

In this paper the geometrically nonlinear equations of motion for anisotropic shells of arbitrary geometry are obtained. On the basis of these equations the axisymmetric deformation of conical and cylindrical shells subjected at the end to axial compressive impact by perfectly rigid mass is investigated. Two phases of the buckling process are distinguished and the dependence of the critical time on a namber of variable parameters is shown. The results of experiments performed for longitudinally corrugated cylindrical shells are presented.

1. Equations of motion

It is assumed that principal directions of elasticity associated with physical or strucutral anisotropy coincide with the directions of the principal curvatures of the middle surface. Assuming in this case constant thickness of the shell and using geometrically nonlinear equations of the three-dimensional theory of elasticity and the Love-Kirhchoff hypothesis together with Timoshenko's correction, the following equations of motion may be obtained:

$$(1.1)\qquad A_1 A_2 \ddot{u} = \frac{\partial}{\partial \xi_1}(A_2 \overset{*}{\varepsilon}_{11}) + \frac{\partial}{\partial \xi_2}(A_1 \overset{*}{\varepsilon}_{21}) + \overset{*}{\varepsilon}_{12}\frac{\partial A_1}{\partial \xi_2} - \overset{*}{\varepsilon}_{22}\frac{\partial A_2}{\partial \xi_1} - A_1 A_2 \frac{\overset{*}{\varepsilon}_{13}}{R_1},$$

$$A_1 A_2 \ddot{v} = \frac{\partial}{\partial \xi_1}(A_2 \varepsilon_{12}^*) + \frac{\partial}{\partial \xi_2}(A_1 \varepsilon_{22}^*) + \varepsilon_{21}^* \frac{\partial A_2}{\partial \xi_1} - \varepsilon_{11}^* \frac{\partial A_1}{\partial \xi_2} - A_1 A_2 \frac{\varepsilon_{23}^*}{R_2}, \tag{1.2}$$

$$A_1 A_2 \ddot{w} = \frac{\partial}{\partial \xi_1}(A_2 \varepsilon_{13}^*) + \frac{\partial}{\partial \xi_2}(A_1 \varepsilon_{23}^*) + A_1 A_2 \left(\frac{\varepsilon_{11}^*}{R_1} + \frac{\varepsilon_{22}^*}{R_2}\right), \tag{1.3}$$

$$A_1 A_2 \ddot{\alpha} = -\frac{\partial}{\partial \xi_1}(A_2 \chi_{11}^*) - \frac{\partial}{\partial \xi_2}(A_1 \chi_{21}^*) - \chi_{12}^* \frac{\partial A_1}{\partial \xi_2} + \chi_{22}^* \frac{\partial A_2}{\partial \xi_1} + \chi_{13}^* \frac{A_1 A_2}{R_1} + 12\varepsilon_{31}^* \frac{A_1 A_2}{h^2}, \tag{1.4}$$

$$A_1 A_2 \ddot{\beta} = -\frac{\partial}{\partial \xi_1}(A_2 \chi_{12}^*) - \frac{\partial}{\partial \xi_2}(A_1 \chi_{22}^*) - \chi_{21}^* \frac{\partial A_2}{\partial \xi_1} + \chi_{11}^* \frac{\partial A_1}{\partial \xi_2} + \chi_{23}^* \frac{A_1 A_2}{R_2} + 12\varepsilon_{32}^* \frac{A_1 A_2}{h^2}. \tag{1.5}$$

In the equations (1.1)–(1.5) the following notations were introduced:

$$\begin{gathered}
\varepsilon_{ik}^* = \varepsilon_{is}^0 \lambda_{sk}, \qquad \chi_{ik}^* = \chi_{is}^0 \lambda_{sk} + \varepsilon_{is}^0 \delta_{sk}, \\
\varepsilon_{11}^0 = \varepsilon_{11} + \mu\eta\varepsilon_{22}, \qquad \varepsilon_{22}^0 = \eta(\varepsilon_{22} + \sigma\varepsilon_{11}), \\
\chi_{11}^0 = \chi_{11} + \mu\eta\chi_{22}, \qquad \chi_{22}^0 = \eta(\chi_{22} + \mu\chi_{11}), \\
\varepsilon_{ik}^0 = 2k_{ik}\varepsilon_{ik} = \varepsilon_{ki}^0, \qquad \chi_{ik}^0 = 2k_{ik}\chi_{ik} = \chi_{ki}^0, \qquad (i \neq k), \\
2\varepsilon_{ik} = e_{ik} + e_{ki} + e_{is}e_{ks}, \qquad 2\chi_{ik} = \psi_{ik} + \psi_{ki} + \psi_{is}\psi_{ks}, \\
\varepsilon_{33} = -\frac{1}{1-\mu^2\eta}\{(\mu_{31} + \mu\eta\mu_{32})\varepsilon_{11} + (\mu_{32} + \mu\eta\mu_{31})\varepsilon_{22}\};
\end{gathered} \tag{1.6}$$

$$\begin{gathered}
e_{ii} = \frac{1}{A_i}\frac{\partial u_i}{\partial \xi_i} + \frac{u_j}{A_i A_j}\frac{\partial A_i}{\partial \xi_j} - \frac{w}{R_i} \qquad (i, j = 1, 2), \\
e_{ij} = \frac{1}{A_i}\frac{\partial u_j}{\partial \xi_i} - \frac{u_i}{A_i A_j}\frac{\partial A_i}{\partial \xi_j} \qquad (i \neq j), \qquad e_{33} = 0, \\
e_{i3} = \frac{1}{A_i}\frac{\partial w}{\partial \xi_i} + \frac{u_i}{R_i}, \qquad e_{3i} = -\alpha_i \qquad (i = 1, 2,);
\end{gathered} \tag{1.7}$$

$$\begin{gathered}
\psi_{ii} = -\frac{1}{A_i}\frac{\partial \alpha_i}{\partial \xi_i} - \frac{\alpha_j}{A_i A_j}\frac{\partial A_i}{\partial \xi_j} \qquad (i, j = 1, 2), \qquad \psi_{3i} = 0 \qquad (i = 1, 2, 3), \\
\psi_{ij} = -\frac{1}{A_i}\frac{\partial \alpha_j}{\partial \xi_i} + \frac{\alpha_i}{A_i A_j}\frac{\partial A_i}{\partial \xi_j} \qquad (i \neq j), \qquad \psi_{i3} = -\frac{\alpha_i}{R_i} \qquad (i = 1, 2), \\
u_1 = u, \qquad u_2 = v, \qquad \alpha_1 = \alpha, \qquad \alpha_2 = \beta;
\end{gathered} \tag{1.8}$$

$$\lambda_{ik}=\delta_i^k+e_{ik}(1-\delta_i^k), \quad \delta_{ik}=\psi_{ik}(1-\delta_i^k),$$
$$k_{12}=k_{21}=(1-\mu^2\eta)G_{12}/E, \quad \mu=\mu_{21}, \quad E=E_1, \tag{1.9}$$
$$k_{i3}=k_{3i}=(1-\mu^2\eta)G_{i3}k_{i3}^0/E, \quad \eta=E_2/E=\mu_{12}/\mu_{21}.$$

Here u, v, w, α and β denote the linear and angular displacements; ρ, E_1, E_2 are the material density and the elastic moduli in the directions ξ_1 and ξ_2; μ_{ik} denote the components of the shear strains in the directions ξ_i during extension (compression) along ξ_k; G_{ik} are the shear moduli in the corresponding planes, η is the anisotropy coefficient (tangential); k_{i3}^0 are the coefficients of tangential stress distribution; A_i, R_i denote Lamé prameters and radii of the principal curvatures of the middle surface; δ_{ik} is the Kronecker symbol. The index "s" in the formulae (1.6) denotes summation from 1 to 3. The arrow brackets indicate the cyclic permutation of the indices, and the dot denotes partial differentiation with respect to time t.

As it is seen, the equations obtained take into account the tangential and normal inertia, transverse shear strain, nonlinear terms in the expressions for ε_{ik} and χ_{ik}, the complementary stresses associated with the rotation of the normal to the middle surface and interaction of all the vibration modes. The metric of shells is assumed to be invariable in a process of deformation. The equations (1.1)–(1.5) are written in a dimensionless form; the linear quantities are referred to the characteristic linear parameter L, which for example, may be the length of the generator, and time t is referred to the period of the shear wave propagation along L:

$$t=c_1T/L \quad (c_1^2=c_0^2/(1-\mu^2\eta), \quad c_0^2=E/\rho). \tag{1.10}$$

Here, T denotes physical time

To compare the shells having various anisotropy coefficients it is convenient to assume the isotropic shell as a standard one and to normalize the time with respect to the period of the wave propagation along the L of the standard shell, i.e. to use in the Eq. (1.10) $c=c_0/\sqrt{1-\mu^2}$ instead of c_1. In this case the right-hand sides of the Eqs. (1.1)–(1.5) should be multiplied by $(1-\mu^2)/(1-\mu^2\eta)$. It is easy to show that when the shells with variable anistoropy coefficient $\eta=\eta(\xi_1,\xi_2)$ are considered, the right-hand sides of the Eqs. (1.1)–(1.5) should be complemented by the following terms (t is normalized with respect to c).

$$+D\left\{A_2\varepsilon_{1k}^*\frac{\partial}{\partial\xi_1}+A_1\varepsilon_{2k}^*\frac{\partial}{\partial\xi_2}\right\}\eta \quad (k=1,2,3),$$
$$-D\left\{A_2\chi_{1k}^*\frac{\partial}{\partial\xi_1}+A_1\chi_{2k}^*\frac{\partial}{\partial\xi_2}\right\}\eta \quad (k=1,2), \tag{1.11}$$
$$\left(D=\frac{\mu^2(1-\mu^2)}{(1-\mu^2\eta)^2}\right).$$

The first three expressions are referred to the Eqs. (1.1)–(1.3) while the second two expressions — to the Eqs. (1.4)–(1.5).

2. Axisymmetric buckling of conical and cylindrical shells

The axially symmetric deformation of conical and cylindrical shells was analyzed numerically by means of the digital computer "Minsk-22". The equations of motion and the basic relations were obtained from the Eqs. (1.1)–(1.9) under assumption

$$v \equiv 0, \quad \beta \equiv 0, \quad \partial/\partial\xi_2 \equiv 0. \tag{2.1}$$

Besides for the conical shells we assumed additionally

$$\begin{aligned} &A_1 = 1, \quad A_2 = R + \xi \sin\varphi \quad (\xi = \xi_1), \\ &1/R_1 = 0, \quad 1/R_2 = \cos\varphi / A_2. \end{aligned} \tag{2.2}$$

Here R is the radius of the middle surface in the end cross-section absorbing impact 2φ is the angle of conicity.

Integration of the corresponding equations of motion was achieved for the following initial and boundary conditions:

$$\begin{aligned} &u=0, \quad \dot{u} = V\cos\varphi \quad (\xi=0), \quad \dot{u}=0 \quad (0<\xi\leqslant 1) \\ &w=0, \quad \dot{w} = V\sin\varphi \quad (\xi=0), \quad \dot{w}=0 \quad (0<\xi\leqslant 1) \\ &\qquad \alpha=0, \quad \dot{\alpha}=0 \quad \text{for} \quad t=0; \end{aligned} \tag{2.3}$$

$$\begin{aligned} &(\partial^2/\partial t^2 - \kappa\partial/\partial\xi)\, u = 0, \quad w = u \operatorname{tgn}\varphi, \quad \alpha=0 \quad \text{for} \quad \xi=0, \\ &u=0, \quad w=0, \quad \alpha=0 \quad \text{for} \quad \xi=1 \left(\kappa = \frac{M_0}{M}\right). \end{aligned} \tag{2.4}$$

Assuming $\varphi=0$ in the Eqs. (2.2)–(2.4) the corresponding equations for cylindrical shells are obtained.

The equations of motion together with the initial and boundary conditions were converted into difference form. The explicit scheme of the standard difference method without analysis of the discontinuities was applied [20]. The derivatives were replaced by the first order central differences. The values of the functions in the mesh points lying outside the boundary were evaluated from the simultaneous consideration of the corresponding equations of motion and initial or boundary conditions. The choice of the mesh ratio ensuring stability of the method and convergence of the computing process is based on the results of paper [21]. The majority of computations were performed assuming $s=1/40$ and $\tau=1/160$ (s and τ are space and time increments).

In Fig. 1 the results of computations of the impact buckling for cylindrical shells are presented. In this case $V=0.06$, $\kappa=0$, $\eta=0.1$, $R=0.3$ and $h=0.02$. In particular the distributions of the axial and radial displacements u and w (configurations of the elastic surface for the isotropic shell $\eta=1$ are marked by dots), the dimensionless curves of axial (ε_{11}^0) and circumferential (ε_{22}^0) strains and bending moment (χ_{11}^0) are presented at successive instants of time. In real scale u — 0.20, w — 0.04, ε_{11}^0 — 0.20, ε_{22}^0 — 0.02 and χ_{11}^0 — 20.00. It is obvious that the general picture of the impact

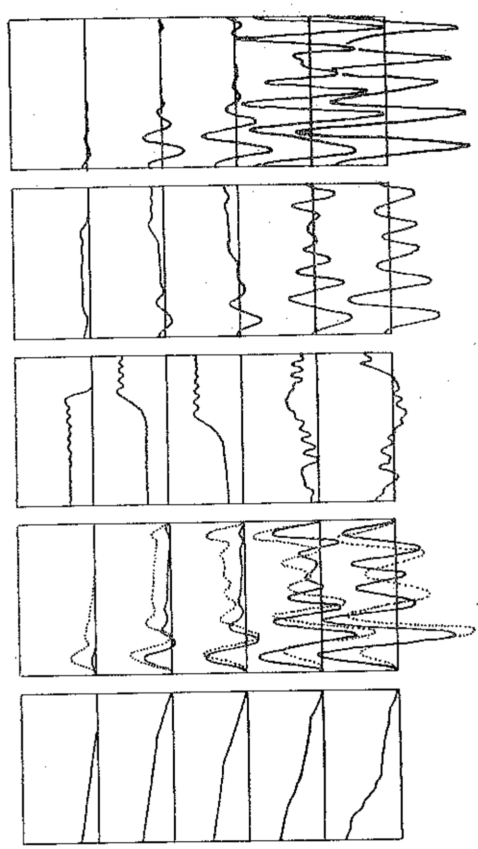

FIG. 1. Development of axisymmetric deformation in cylindrical shell.

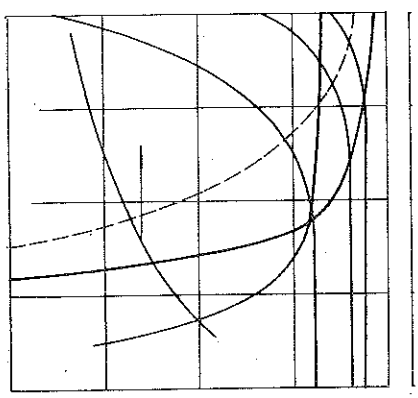

FIG. 2. Dependence of t_* on R, V, h and η for cylindrical shell.

buckling is analogous to the buckling of isotropic shells described in papers [22] and [23]. Similarly to the case of isotropic shells the process of buckling impact may be conventionally divided into two phases subcritical and postcritical. During the first phase, the comparatively slow and monotone buckling of the shell in the direction of the external normal is observed. In addition, the unique halfwave arising after the impact in the disturbed zone is seen. The influence of the geometrical nonlinearity is practically negligible.

The second phase is concerned with further complication of the configuration of the elastic surface and with the sharp increase in the speed of growth of deflections. The nonlinearity in this stage shows very essential influence on the all parameters characterizing the impact deformation process in the shell. The objective boundary dividing the subcritical and postcritical phases is determined by the critical time which is defined as the moment of snap-through of the shell toward the interior. This snap through leads to the stable transformation of dynamic forms of the elastic surface.

The dependence of the critical time t_* on the several variable parameters is depicted in Fig. 2. The curve 1 represents the function $t_*(R)$ ($\eta=0.25$, $V=0.04$). It is seen that for $R>0.75$ the critical time is practically invariable. The curves *2* and *3* represent the function $t_*(V)$ for $\eta=0.25$ and $\eta=1.00$, respectively ($R=0.3$), while the curves *4*, *5* and *6* represent the function $t_*(\eta)$ for various impact velocities: $V=0.04$, 0.06 and 0.08. It is noteworthy that at $\eta<0.1$ the critical time is almost independent of the anisotropy coefficient. The relation $t_*(h)$ is given by the curve *7* ($\eta=0.1$, $V=0.06$). The variation in time of the integral parameters characterizing buckling process of the shell is shown in Fig. 3 ($V=0.03$, $\eta=0.1$, $\kappa=0$, $R=0.3$ and $h=0.02$):

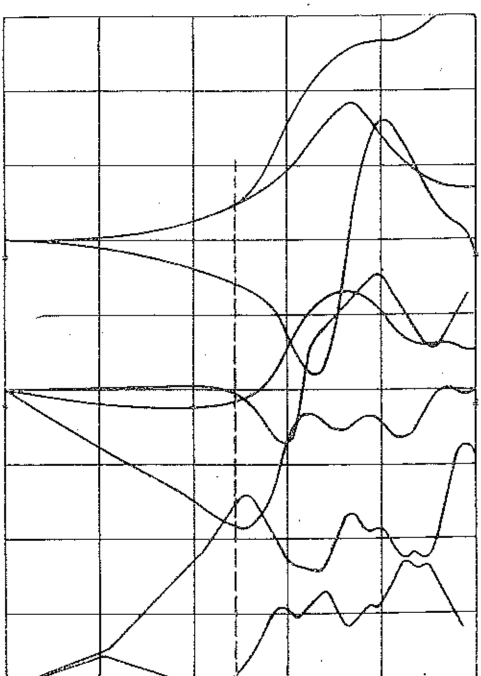

FIG. 3. Time variations of integral parameters and energy (cylindrical shell, $\kappa=0$).

$$(2.5)\qquad \{f_+, f_-, \dot{f}, \varepsilon_{ii}^0, \chi_{11}^0\} = \int_0^1 \{|w(\xi,t)|, w(\xi,t), \dot{w}(\xi,t), \varepsilon_{ii}^0(\xi,t), \chi_{11}^0(\xi,t)\}\, d\xi .$$

The vertical dashed line denotes the critical time $t_*\approx 2.45$ and T is the shell energy. The curves *1–3* represent, respectively, the functions $f_+(t)$, $f_-(t)$ and $\dot{f}(t)$ ($f_-(t)$ was traced with opposite sign); the curves *4–6* characterize arising in shell the bending, circumferencial and axial stresses. The curves *7* and *8* show the variation of the potential and kinetic energies. It is seen that after transformation of the dynamic forms ($t > t_*$) the absolute values of the all parameters rapidly increase. The axial stresses (curve *6*) and potential energy (*7*) are the exceptions. They initially decrease and then start to oscillate. These oscillations express evidently the nonlinear effects. The decay of the axial stresses at the postcritical state of buckling, shown here (probably the first time) indicate the exhaustion of the carrying capacity of the shell and, of course, may be treated as the loss of stability under axial impact. From this Figure the peculiar behaviour of the dimensionless energy (T_p, T_k) is also seen

$$(T_p, T_k) = (E_p, E_k)/(M_0\, c_2/2). \tag{2.6}$$

E_p and E_k denote here physical values of the potential and kinetic energies. Together with the computation of the energy of the system the particular energy components were also evaluated. It was found that in a subcritical buckling stage the energy of tangential extension — compression brings the main contribution to the potential energy of the shell. At $t=0.2$ this energy, in the case considered, constitutes more than 99.8% of the entire potential energy. The bending and shear energies make respectively 0.11% and less than 0.02%. At the postcritical phase the bending and shear energies increase and at $t=4.8$ the energy components are equal to 72.48%, 24.00% and 3.52%, respectively. The energy of the axial motions constitutes the main part of the kinetic energy at the subcritical stage, namely more than 99.76% at $t=1.0$. At $t=4.8$ the fractions of the energy of axial, radial and rotational motions 42.29%, 56.98% and 0.73%, respectively. Thus during all buckling stages the energy accumulated by shear and rotation constitutes negligible part of the total shell

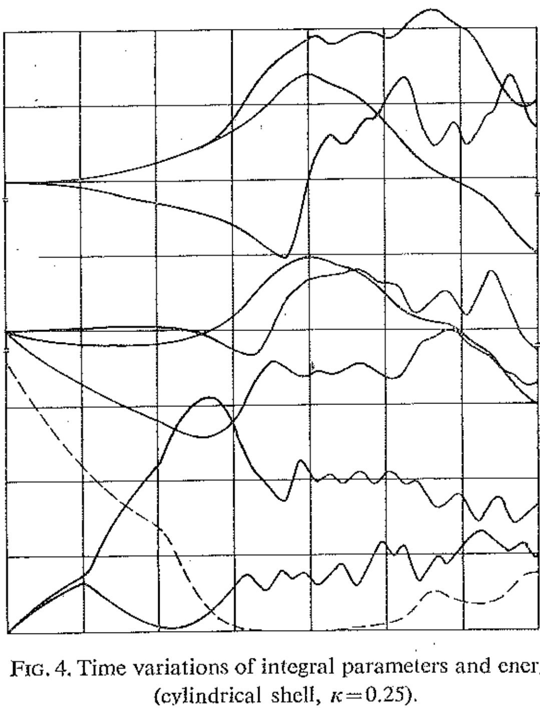

FIG. 4. Time variations of integral parameters and energy (cylindrical shell, $\kappa=0.25$).

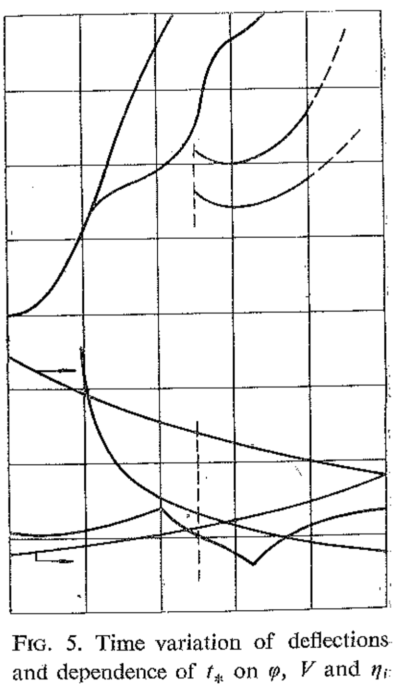

FIG. 5. Time variation of deflections and dependence of t_* on φ, V and η_i ($i=1, 2$) for conical shell.

energy. The analogous relations with taking into account the mass of the shell are shown in Fig. 4 ($\kappa=0.25$, the remaining parameters are unchanged). The dashed curve describes kinetic energy of the impact load.

As a second example of the application of the equations derived we consider the impact buckling of orthotropic conical shells with the anisotropy coefficient assumed constant and varying linearly along the generator. The main results are presented in Fig. 5. The curves *1–4* refer to conical shell with $\eta=\text{const}$. The curves *1* ($\varphi=50°$) and *2* ($\varphi=40°$, $V=0.06$, $R=0.25$, $h=0.05$ and $\eta=0.1$) represent the function $f_r(t)$. The relation $t_*(\varphi)$ for the isotropic and anisotropic shells is shown illustrated by curves *3* and *4*. The functions $t_*(V)$ ($\varphi=30°$) and $t_*(\varphi)$ ($V=0.06$) for $\eta_1=0.01$ and $\eta_2=1.00$ (η_1 and η_2 are the values of the coefficient η at the impacted and not impacted end, respectively) are shown in curves *5* and *6*. Distributions of the functions $t_*(\eta_1)$ ($\eta_2=1$) and $t_*(\eta_2)$ ($\eta_1=1$; $V=0.06$, $\varphi=30°$) are demonstrated in curves *7* and *8*. The general character of deformation of the conical shell is analogous to the previous case.

3. Experiments on corrugated cylindrical shells

The experiments on the impact loading of shells were performed on the special stand with falling load. The high-speed camera SKS-1m having the speed of about 4000 shots per second and the measuring microscope from the "Pentacet" set were used for registration of the data. The weight of the load varied from 250 g to 10 kg and the impact velocity reached up to 10 m/sec. The shells with longitudinal corrugation were prepared by folding and glueing corrugated aluminium layers by the epoxy resin ($h=0.25$ mm, $h_0\approx2.0$, $l_0\approx4.0$ mm, where h_0 and l_0 denote the amplitude and the wave length of the corrugation). The corrugation profile is almost sinusoidal. The radius and working height of the shell were equal to 57 mm and 190 mm, respectively. The elastic modulus in the annular direction $E_2\approx17640$ kg/cm^2 (obtained from measuring) and the anisotropy coefficient $\eta\approx0.025$.

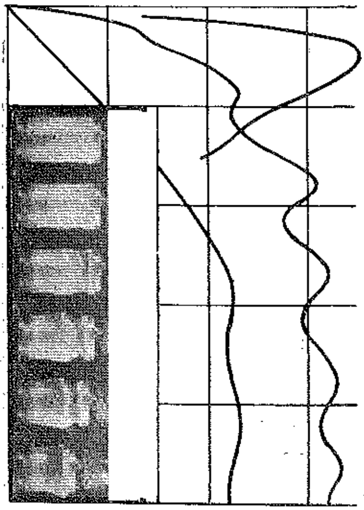

Fig. 6. Experimental results.

In Fig. 6 the set of pictures is presented (the numbers are the consecutive numbers of the shots. The curves *1* and *2* show the variation of the internal and external amplitude of the halfwaves, the curve *3* gives the rule of approaching of the ends of shell.

It is seen that initially the impacted end moves simultaneously with the load (the lower end is clamped to the massive plate of foundation). Then the load is stopped and leaped off while the upper end of the shell starts to experience the axial vibrations. The moment of separation of the load and the end corresponds to 50–55-th photograph ($t \approx 0.0125$ sec, it is missing in the shots). The amplitude of radial vibrations of the external half-wave arise much earlier and may be observed already from the 5-th shot. It is characteristic that the frequency of radial vibrations is approximately two times higher than the frequency of axial vibrations. The peculiar character of the impact deformation of the corrugated shells is clearly seen in the picture presented in Fig. 7 (the left-hand side shell is after static compression).

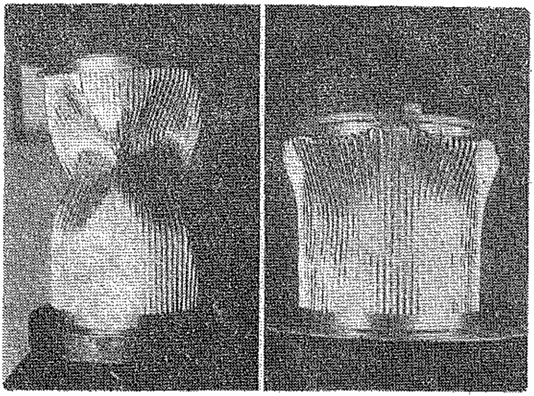

FIG. 7. Computational results for statical and impact compression of corrugated shells.

In conclusion we should like to stress that in spite of the investigation performed the problem of behaviour of the corrugated and anisotropic shells under axial impact is still far from the final solution. In this domain further development of theoretical studies and perfectioning the experimental measuring techniques is desired.

REFERENCES

1. S. G. LECHNICKI, *Anisotropic plates*, Gos. Tech. Izdat., Moscow, 1947 [in Russian].
2. M. T. HUBER, *Theory of elasticity*, PWN, Warsaw, 1950 (in Polish).
3. A. SAWCZUK, *Some problems of load carrying capacities of orthotropic and nonhomogeneous plates*, Arch. Mech. Stos., **8**, 4, 1956.
4. A. SAWCZUK, *Linear theory of plasticity of anisotropic bodies*, Arch. Mech. Stos., **11**, 5, 1959.
5. S. A. AMBARTSUMIAN, *Theory of anisotropic shells*, Fiz. Mat. Giz, Moscow, 1961 [in Russian].
6. S. A. AMBARTSUMIAN, *Theory of anisotropic plates*, Nauka, Moscow, 1967 [in Russian].
7. V. V. BOLOTIN, *On the theory of reinforced media*, Mechanics, 1, 1965. [in Russian].
8. V. V. BOLOTIN, *Basic equations of the theory of reinforced media*, Mechanics of Polymers, 2, 1965 [in Russian].
9. V. V. BOLOTIN and V. N. MOSKALENKO, *Plates and shells made of reinforced materials — basic equations, quantitative results*, Collection of lectures of the Scientific-Technological Conference on the Results of Scientific Investigations in 1966–1967, MEI, Moscow, 1967 [in Russian].
10. D. L. PLATUS, and S. UCHIGAMA, *Very large deflection behaviour of corrugated strips*, AIAA Journal, **3**, 8, 1965.
11. A. K. KALLINIS, *On the refinement of the equation of motion for thermoelastic orthotropic shells*, "Investigations on the theory of plates and shells", **8**, Kazan, 1972 [in Russian].
12. L. N. SMETANINA, *Nonlinear problems of dynamic stability of orthotropic shell under external transverse pressure*, Collection of Ph. D. Theses of the Voronezh Forestial Technological Institute, 2, 1965 [in Russian].

13. A. A. Bushtyrkov, and A. A. Naida, *Dynamic behaviour of thin-walled cylindrical shells made of anisotropic elastic materials under transient external pressure*, Theses of Lectures on the 4-th National Conference on the Problems of Stability and Structural Mechanics (Kharkov 1972), Moscow 1972 [in Russian].
14. A. A. Naida and V. K. Ovchinnikov, *Response of plastic-glass cylindrical shell to the action of the explosive load*, Appl. Mechanics, 12, 8, 1972 [in Russian].
15. L. A. Movsisian, *Longitudinal impact on the cylindrical shell*, Izv. A. N. Arm. SSR, **17**, 6, 1964 [in Russian].
16. L. A. Movsisian, *Stability of cylindrical shells under impact loading*. Theses of Lectures on the 4-th National Conference on the Problems of Stability and Structural Mechanics (Kharkov 1972), Moscow 1972 [in Russian].
17. V. C. Grunin and L. A. Movsisian, *Longitudinal impact of the anisotropic semi-infinite cylindrical shell of revolution on the rigid wall*, "Transient Processes of Deformation of Shells and Plates", Tallin 1967 [in Russian].
18. V. L. Agamirov and L. N. Smetanina, *Experimental investigation of stability of cylindrical shells under longitudinal impact*, Theses of Lectures of 5-th National Conference on Theory of Plates and Shells, Moscow 1965 [in Russian].
19. B. A. Gordienko and L.D. Shevchyk, *Behaviour of corrugated shells in conditions of impulsive loading*, Thesee of Lectures on the 4-th National Conference on the Problems of Stability and Structural Mechanics (Kharkov 1972), Moscow 1972 [in Russina].
20. U. K. Nigul and J. K. Engelbrecht, *Nonlinear and linear transient wave processes of deformation of thermoelastic and elastic bodies*, Tallin 1972 [in Russian].
21. B. A. Gordienko, *On the numerical solution of the impact buckling problems of elastic systems by the method of finite differences*, Mechanics of Solids, Izv. AN SSSR, 3, 1970 [in Russian].
22. B. A. Gordienko, *Behaviour of cylindrical shells under axial impact*, Collected Works of Chabarovsk Politechnical Institute, Ed. 25, Chabarovsk 1971 [in Russian].
23. B. A. Gordienko, *Impact buckling of elastic systems*, Mechanics of Solids, 4, Izv. AN SSSR, 1974 [in Russian].

Streszczenie

ANALIZA DEFORMACJI POMARSZCZONYCH I ANIZOTROPOWYCH POWŁOK PODDANYCH OSIOWEMU UDERZENIU

Istnienie anizotropii materiału przy $E_2/E_1 < 1$ powłok obciążonych uderzeniowo obniża czas krytyczny i prowadzi do powstania osiowo-symetrycznych postaci wyboczenia. Dane doświadczeń przeprowadzonych na wzdłużnie pomarszczonych powłokach pokrywają się z wynikami badań teoretycznych.

Резюме

ИССЛЕДОВАНИЕ УДАРНОГО ДЕФОРМИРОВАНИЯ ГОФРИРОВАННЫХ И АНИЗОТРОПНЫХ ОБОЛОЧЕК

Наличие анизотропии материала (при $E_2/E_1 < 1$) для ударно нагруженных оболочек снижает критическое время и способствует развитию осесимметричных форм выпучивания. Данные экспериментов с продольно гофрированными оболочками находятся в удовлетворительном соответствии с результатами теоретических исследований.

Received April 3, 1976.